

NO-A198 296

A POSTERIORI ERROR ESTIMATION IN A FINITE ELEMENT
METHOD FOR PARABOLIC P.D. (U) ARMY ARMAMENT RESEARCH
DEVELOPMENT AND ENGINEERING CENTER WAT.

1/1

UNCLASSIFIED

J H COYLE ET AL. DEC 87 ARCCB-TR-87037

F/G 12/1

ML





AD-A190 296

DTIC FILE COPY

AD

TECHNICAL REPORT ARCCB-TR-87037

**A POSTERIORI ERROR ESTIMATION
IN A FINITE ELEMENT METHOD FOR
PARABOLIC PARTIAL DIFFERENTIAL EQUATIONS**

J.M. COYLE

J.E. FLAHERTY

DTIC
ELECTE
FEB 17 1988
S H D

DECEMBER 1987



**US ARMY ARMAMENT RESEARCH, DEVELOPMENT
AND ENGINEERING CENTER
CLOSE COMBAT ARMAMENTS CENTER
BENÉT WEAPONS LABORATORY
WATERVLIET, N.Y. 12189-4050**

APPROVED FOR PUBLIC RELEASE; DISTRIBUTION UNLIMITED

88 2 11 099

DISCLAIMER

The findings in this report are not to be construed as an official Department of the Army position unless so designated by other authorized documents.

The use of trade name(s) and/or manufacturer(s) does not constitute an official indorsement or approval.

DESTRUCTION NOTICE

For classified documents, follow the procedures in DoD 5200.22-M, Industrial Security Manual, Section II-19 or DoD 5200.1-R, Information Security Program Regulation, Chapter IX.

For unclassified, limited documents, destroy by any method that will prevent disclosure of contents or reconstruction of the document.

For unclassified, unlimited documents, destroy when the report is no longer needed. Do not return it to the originator.

REPORT DOCUMENTATION PAGE		READ INSTRUCTIONS BEFORE COMPLETING FORM
1. REPORT NUMBER ARCCB-TR-87037	2. GOVT ACCESSION NO.	3. RECIPIENT'S CATALOG NUMBER AD-A190296
4. TITLE (and Subtitle) A POSTERIORI ERROR ESTIMATION IN A FINITE ELEMENT METHOD FOR PARABOLIC PARTIAL DIFFERENTIAL EQUATIONS		5. TYPE OF REPORT & PERIOD COVERED Final
7. AUTHOR(s) J. M. Coyle and J. E. Flaherty (See Reverse)		6. PERFORMING ORG. REPORT NUMBER
9. PERFORMING ORGANIZATION NAME AND ADDRESS US Army ARDEC Benet Laboratories, SMCAR-CCB-TL Watervliet, NY 12189-4050		8. CONTRACT OR GRANT NUMBER(s)
11. CONTROLLING OFFICE NAME AND ADDRESS US Army ARDEC Close Combat Armaments Center Picatinny Arsenal, NJ 07806-5000		10. PROGRAM ELEMENT, PROJECT, TASK AREA & WORK UNIT NUMBERS AMCMS No. 6920.OR.8970.021 PRON No. 1A62ZHFCNMLC
14. MONITORING AGENCY NAME & ADDRESS (if different from Controlling Office)		12. REPORT DATE December 1987
		13. NUMBER OF PAGES 23
		15. SECURITY CLASS. (of this report) UNCLASSIFIED
		15a. DECLASSIFICATION/DOWNGRADING SCHEDULE
16. DISTRIBUTION STATEMENT (of this Report) Approved for public release; distribution unlimited.		
17. DISTRIBUTION STATEMENT (of the abstract entered in Block 20, if different from Report)		
18. SUPPLEMENTARY NOTES Presented at the Fourth Army Conference on Applied Mathematics and Computing, Cornell University, Ithaca, New York, 27-30 May 1986. Published in Proceedings of the Conference.		
19. KEY WORDS (Continue on reverse side if necessary and identify by block number) Error Estimation Finite Element Method Superconvergence Backward Euler Method Mesh Refinement Trapezoidal Rule		
20. ABSTRACT (Continue on reverse side if necessary and identify by block number) Superconvergence properties and quadratic polynomials are used to derive a computationally inexpensive approximation to the spatial component of the error in a piecewise linear finite element method for one-dimensional parabolic partial differential equations. This technique is coupled with time integration schemes of successively higher orders to obtain an approximation of the temporal and total discretization errors. Computational results indicate that these approximations converge to the exact discretization errors as the mesh is (CONT'D ON REVERSE)		

7. AUTHORS (CONT'D)

J. E. Flaherty
 Department of Computer Science
 Rensselaer Polytechnic Institute
 Troy, NY 12180-3590

and

US Army ARDEC
 Close Combat Armaments Center
 Benet Laboratories
 Watervliet, NY 12189-4050

20. ABSTRACT (CONT'D)

→ refined. The approximate errors are used to control an adaptive mesh refinement strategy.

Control *trapezoidal rule*

method

Accession For	
NTIS GRA&I	<input checked="" type="checkbox"/>
DTIC TAB	<input type="checkbox"/>
Unannounced	<input type="checkbox"/>
Justification	
By	
Distribution/	
Availability Codes	
Avail and/or	
Dist	Special
A-1	

UNCLASSIFIED

TABLE OF CONTENTS

	<u>Page</u>
INTRODUCTION.	1
DISCRETE SYSTEM	3
Spatial Discretization	4
Temporal Discretization	5
ERROR ESTIMATION	6
MESH REFINEMENT	11
DISCUSSION	16
REFERENCES	18

TABLES

I. NUMERICAL PARAMETERS AT THE BEGINNING AND THE END OF EACH TIME STEP FOR SOLVING EXAMPLE 2 WITH TOL = 0.2.	15
II. NUMERICAL PARAMETERS AT THE BEGINNING AND THE END OF EACH TIME STEP FOR SOLVING EXAMPLE 2 WITH TOL = 0.1.	15
III. NUMERICAL PARAMETERS AT THE BEGINNING AND THE END OF EACH TIME STEP FOR SOLVING EXAMPLE 2 WITH TOL = 0.5.	16

LIST OF ILLUSTRATIONS

1. Reciprocal of the effectivity index θ versus p , where $N = 2^{p+1}$ and $\Delta t = 5^{-p/2}$ when solving Example 1.	20
2. Temporal effectivity index θ_t for $\Delta t = 0.7$ (curve 1), $\Delta t = 0.49$ (curve 2), $\Delta t = 0.343$ (curve 3), and $\Delta t = 0.2401$ (curve 4), versus p , where $N = 2^p$ when solving Example 1.	21
3. Reciprocal of the spatial effectivity index θ_s for $N = 2$ (curve 1), $N = 4$ (curve 2), and $N = 8$ (curve 3) versus p , where $\Delta t = 5^{-p/2}$ when solving Example 1.	22

INTRODUCTION

Adjerid and Flaherty (refs 1,2) developed an a posteriori estimate of the spatial discretization error in a finite element method of lines for solving vector systems of parabolic partial differential equations. They discretized the system in space using Galerkin's method with piecewise linear finite element approximations. The error estimate was calculated using Galerkin's method with piecewise quadratic functions. A nodal superconvergence property of the finite element method was used to neglect errors at nodes and, thus, improve computational efficiency. Ordinary differential equations (ODE's) for the finite element solution and error estimate were then integrated in time using the backward difference code DASSL (ref 3).

Adjerid and Flaherty (refs 1,2) assumed that the temporal discretization error associated with DASSL was negligible compared to the spatial error. Thus, their estimate of the spatial discretization error could be regarded as an estimate of the total error. They used their error estimate to control mesh moving and local mesh refinement procedures that attempted to equidistribute the error estimate and satisfy a prescribed global error tolerance. Similar mesh refinement strategies have been used by Bieterman and Babuska (refs 4,5).

Our goal is to develop techniques that simultaneously estimate the temporal and spatial discretization errors. To this end, we consider M-dimensional partial differential systems of the form

$$u_t(x,t) + f(x,t,u,u_x) = (D(x,t)u_x(x,t))_x, \quad a < x < b, \quad t > 0, \quad (1a)$$

subject to the initial conditions

$$u(x,0) = u^0(x), \quad a \leq x \leq b, \quad (1b)$$

References are listed at the end of this report.

and boundary conditions

$$\begin{aligned}A_L(t)u(a,t) + B_L(t)u_x(a,t) &= g_L(t) , \\A_R(t)u(b,t) + B_R(t)u_x(b,t) &= g_R(t) , \quad t > 0 .\end{aligned}\tag{1c}$$

The variables x and t represent spatial and temporal coordinates and denote partial differentiation when they are used as subscripts; u , f , u^0 , g_L , and g_R are M -vectors, and D , A_L , B_L , A_R , and B_R are $M \times M$ matrices.

We, like Adjrid and Flaherty (refs 1,2), discretize Eq. (1) in space using Galerkin's method with piecewise linear finite elements. Temporal discretization, however, is performed by the backward Euler method as opposed to using an ODE code. A second solution is calculated using trapezoidal rule integration in time and the difference between the two solutions is used to furnish an estimate of the temporal discretization error. A third solution is obtained using Adjrid and Flaherty's (refs 1,2) quadratic finite elements and the trapezoidal rule in time. This solution is higher order in space and time than the original piecewise linear finite element-backward Euler solution. Hence, it can be used to provide an estimate of the total discretization error of the piecewise linear finite element-backward Euler solution. Furthermore, the difference between the piecewise linear and quadratic solutions calculated by the trapezoidal rule can be used to furnish an estimate of the spatial discretization error.

At first sight, the above procedure seems to be very expensive; however, nodal superconvergence significantly reduces computational complexity. Defect correction methods can also be used to reduce costs associated with the temporal integration.

The estimates of the temporal, spatial, and total discretization errors of the piecewise linear finite element-backward Euler solution are used to control a global refinement procedure that attempts to keep an estimate of the total

discretization error per time step in H^1 below a prescribed limit. Depending on the proportions of the temporal and spatial error estimates to the total error estimate, we refine the time step, finite element mesh, or both.

The piecewise linear and quadratic finite element procedures and the temporal integration schemes are described in the following paragraphs, as well as the error estimation procedures. Adjerd and Flaherty (ref 6) proved that their spatial error estimate converges to the exact error as the mesh is refined when temporal integration is exact for linear parabolic problems. Similar results have not yet been established when temporal errors are present; however, the computational results shown indicate that convergence of our temporal, spatial, and total error estimates are likely. Our global refinement strategy is then presented, and it is applied to an unstable heat conduction problem. Finally, we discuss our results and suggest some future investigations.

DISCRETE SYSTEM

We simplify the presentation slightly by assuming that only Dirichlet data are prescribed; thus, $B_L(t) = B_R(t) = 0$, $t > 0$, in Eq. (1c). A weak form of Eq. (1) is then constructed by multiplying Eq. (1a) by a test function $v(x,t) \in H_0^1$, integrating the result with respect to x from a to b , and integrating the diffusive term by parts to obtain

$$(v, u_t) + (v, f) + A(v, u) = 0 \quad , \quad t > 0 \quad , \quad \text{for all } v \in H_0^1 . \quad (2a)$$

The inner product (v, u) and strain energy $A(v, u)$ are defined as

$$(v, u) = \int_a^b v^T u dx \quad , \quad A(v, u) = \int_a^b v_X^T D u_X dx . \quad (2b, c)$$

Functions v belonging to H_0^1 are required to have finite values of (v, v) and (v_X, v_X) and vanish at $x = a$ and b . Any weak solution $u \in H_E^1$ of Eq. (2a) must also satisfy the Dirichlet (essential) boundary conditions

$$u(a,t) = A_L^{-1}(t)g_L(t) \quad , \quad u(b,t) = A_R^{-1}(t)g_R(t), \quad t > 0 \quad , \quad (2d,e)$$

and initial conditions obtained by multiplying Eq. (1b) by v and integrating with respect to x , i.e.,

$$(v,u) = (v,u^0) \quad , \quad t = 0 \quad , \quad \text{for all } v \in H_0^1 \quad . \quad (2f)$$

A discrete version of the weak system, Eq. (2), is constructed by using finite element-Galerkin procedures in space and finite difference techniques in time, as follows.

Spatial Discretization

In order to discretize Eq. (2a) in space, we introduce a partition

$$\Pi_N := \{a = x_0 < x_1 < \dots < x_N = b\} \quad (3)$$

of (a,b) into N subintervals (x_{i-1}, x_i) , $i = 1, 2, \dots, N$, and approximate u and v by piecewise polynomial functions U and V , respectively, with regard to this partition. Thus, the spatially-discrete form of Eq. (2) consists of finding $U \in S_E^{N,1}$ such that

$$(V, U_t) + (V, f) + A(V, U) = 0 \quad , \quad t > 0 \quad , \quad \text{for all } V \in S_0^{N,1} \quad , \quad (4a)$$

$$(V, U) = (V, u^0) \quad , \quad t = 0 \quad , \quad \text{for all } V \in S_0^{N,1} \quad . \quad (4b)$$

The spaces S_E^N and S_0^N will be chosen to consist of either piecewise linear or piecewise quadratic polynomial functions. The spaces of piecewise linear polynomials are denoted as $S_E^{N,1}$ and $S_0^{N,1}$ and are easily constructed in terms of the familiar "hat" functions

$$\begin{aligned} \phi_i(x) &= \begin{cases} \frac{x - x_{i-1}}{x_i - x_{i-1}} & , \quad x_{i-1} \leq x < x_i \\ \frac{x_{i+1} - x}{x_{i+1} - x_i} & , \quad x_i \leq x < x_{i+1} \\ 0 & , \quad \text{otherwise} \end{cases} \quad , \quad i = 0, 1, \dots, N \quad . \end{aligned} \quad (5)$$

The piecewise linear finite element solution $U^1 \in S_E^{N,1}$ is written in the form

$$U^1(x, t) = \sum_{i=0}^N c_i(t) \phi_i(x) \quad (6)$$

and determined by solving the ordinary differential system

$$(V^1, U^1_t) + (V^1, f) + A(V^1, U^1) = 0, \quad t > 0, \quad \text{for all } V^1 \in S_0^{N,1}, \quad (7a)$$

$$(V^1, U^1) = (V^1, u^0), \quad t = 0, \quad \text{for all } V^1 \in S_0^{N,1}, \quad (7b)$$

where the piecewise linear test functions $V^1 \in S_0^{N,1}$ have a form similar to Eq. (6).

Piecewise quadratic approximations $U^2 \in S_E^{N,2}$ are constructed by adding a "hierarchical" correction $E^2(x, t)$ to U^1 , i.e.,

$$U^2(x, t) = U^1(x, t) + E^2(x, t) \quad (8a)$$

where

$$E^2(x, t) = \sum_{i=1}^N d_{i-\frac{1}{2}}(t) \psi_{i-\frac{1}{2}}(x). \quad (8b)$$

The basis $\psi_{i-\frac{1}{2}}(x)$, $i = 1, 2, \dots, N$, for the quadratic correction has the form

$$\psi_{i-\frac{1}{2}}(x) = \begin{cases} -2 \left(\frac{x - x_{i-1}}{x_i - x_{i-1}} \right) \left(\frac{x_i - x}{x_i - x_{i-1}} \right), & x_{i-1} \leq x \leq x_i \\ 0, & \text{otherwise} \end{cases}, \quad i = 1, 2, \dots, N. \quad (9)$$

Piecewise quadratic solutions are determined by solving

$$(V^2, U^2_t) + (V^2, f) + A(V^2, U^2) = 0, \quad t > 0, \quad \text{for all } V^2 \in S_0^{N,2}, \quad (10a)$$

$$(V^2, U^2) = (V^2, u^0), \quad t = 0, \quad \text{for all } V^2 \in S_0^{N,2}, \quad (10b)$$

where, once again, V^2 has a form similar to Eq. (8).

Temporal Discretization

The finite element systems, Eqs. (4), (7), or (10), are discretized in time for the time step $[t_{n-1}, t_n]$ using a weighted two-step method, which for Eq. (4) has the form

$$(V, \frac{U^n - U^{n-1}}{\Delta t_n}) + \theta[(V, f^n) + A(V, U^n)] +$$

$$(1-\theta)[(V, f^{n-1}) + A(V, U^{n-1})] = 0, \quad \text{for all } V \in S_0^N. \quad (11)$$

The scalar parameter θ is selected on $[0,1]$, $U^n(x) := U(x, t_n)$, etc., and $\Delta t_n := t_n - t_{n-1}$. For simplicity, the test function V has been assumed to be independent of time, although this will not be strictly correct when refinement is incorporated into the finite element method.

The two particular choices of θ that are appropriate for our investigation are $\theta = 1$, which yields the backward Euler method, and $\theta = \frac{1}{2}$, which yields the trapezoidal rule. It is well known (ref 7) that the local discretization error of the backward Euler method is $O(\Delta t_n^2)$ and that of the trapezoidal rule is $O(\Delta t_n^3)$. We will use this difference in the orders of accuracy of the two methods to estimate the local temporal discretization error of the finite element solution.

ERROR ESTIMATION

Local and global estimates of the discretization error have been successfully used to control refinement algorithms that attempt to solve partial differential systems to prescribed levels of accuracy (refs 1,2,4-6,8-12). Our goal is to estimate the discretization error per time step in solutions of Eq. (2) obtained by using piecewise linear finite element approximations in space and the backward Euler method in time. It seems most appropriate to gage errors

$$e := u - U \quad (12)$$

in the H^1 norm

$$\|e\|_1 := [\int_a^b (e_x^T e_x + e^T e) dx]^{\frac{1}{2}} \quad (13)$$

however, other measures may also be used. An error estimate that is global in space and local in time may at first seem unusual, but it is commonly used when spatial finite element approximations are combined with temporal finite difference methods (see Reference 13).

Let the piecewise linear finite element solution obtained by using backward Euler temporal integration be denoted as $U_{BE}^{1,n}(x)$ at time t_n . Likewise, let $U_T^{1,n}(x)$ and $U_T^{2,n}(x)$ denote solutions obtained at t_n by trapezoidal rule integration with piecewise linear and quadratic approximations, respectively.

It is known (ref 14) that $\|u(\cdot, t_n) - U_{BE}^{1,n}(\cdot)\|_1 = O(\Delta t_n^2) + O(\Delta t_n/N)$. Since $\|u(\cdot, t_n) - U_T^{2,n}\|_1 = O(\Delta t_n^3) + O(\Delta t_n/N^2)$, we should be able to use the difference between $U_T^{2,n}$ and $U_{BE}^{1,n}$ to estimate the error in $U_{BE}^{1,n}$; thus,

$$\begin{aligned} \|u - U_{BE}^{1,n}\|_1 &\leq \|U_T^{2,n} - U_{BE}^{1,n}\|_1 + \|u - U_T^{2,n}\|_1 \\ &\leq \|U_T^{2,n} - U_{BE}^{1,n}\|_1 + O(\Delta t_n^3) + O(\Delta t_n/N^2). \end{aligned} \quad (14)$$

The main problem in using $\|U_T^{2,n} - U_{BE}^{1,n}\|_1$ as an a posteriori estimate of $\|u - U_{BE}^{1,n}\|_1$ is the computational effort required to obtain $U_T^{2,n}$. This cost can be reduced considerably by using the superconvergence property of the finite element method for one-dimensional parabolic systems. In the present context, superconvergence implies that finite element solutions converge at a faster rate on Π_N than elsewhere on (a,b) . Hence, the error at the nodes may be neglected relative to the error in the interior of the elements when N is sufficiently large.

Nodal superconvergence has been used by several investigators as a means of constructing a posteriori error estimates in finite element approximations. In particular, Adjerid and Flaherty (refs 1,2) used it in conjunction with their adaptive finite element method of lines. Their situation was somewhat more

restrictive than ours as they also required the temporal error to be negligible relative to the spatial error.

The use of the nodal superconvergence property enables us to approximate $U_T^{2,n}$ as

$$U_T^{2,n} \approx U_T^{1,n} + E_T^{2,n} \quad (15)$$

where $U_T^{1,n}$ is obtained by solving Eq. (7) using trapezoidal rule integration and $E_T^{2,n}$ is obtained by solving Eq. (10a) by trapezoidal rule integration with U^2 replaced by Eq. (15). Furthermore, it is only necessary to test Eq. (10a) against functions $V^2 \in \hat{S}_0^{N,2}$, where $\hat{S}_0^{N,2}$ is a space of quadratic polynomials that vanish on Π_N .

To summarize, our procedure for obtaining the finite element solution $U_{BE}^{1,n}$ and its error estimate $U_T^{1,n} + E_T^{2,n} - U_{BE}^{1,n}$ for the time step $[t_{n-1}, t_n]$ consists of:

- (1) discretizing Eq. (7a) by the backward Euler method and determining $U_{BE}^{1,n}$ as the solution of

$$\begin{aligned} & (V^1, \frac{U_{BE}^{1,n} - U_{BE}^{1,n-1}}{\Delta t_n}) + (V^1, f(\cdot, t_n, U_{BE}^{1,n})) \\ & + A(V^1, U_{BE}^{1,n}) = 0, \text{ for all } V^1 \in S_0^{N,1}, \end{aligned} \quad (16a)$$

- (2) discretizing Eq. (7a) by the trapezoidal rule and determining $U_T^{1,n}$ as the solution of

$$\begin{aligned} & (V^1, \frac{U_T^{1,n} - U_{BE}^{1,n-1}}{\Delta t_n}) + \frac{1}{2} [(V^1, f(\cdot, t_n, U_T^{1,n})) + A(V^1, U_T^{1,n}) \\ & + (V^1, f(\cdot, t_{n-1}, U_{BE}^{1,n-1})) + A(V^1, U_{BE}^{1,n-1})] = 0, \text{ for all } V^1 \in S_0^{N,1}, \end{aligned} \quad (16b)$$

- (3) discretizing Eq. (10a) by the trapezoidal rule and determining $E_T^{2,n}$ as the solution of

$$\begin{aligned}
& (V^2, \frac{U_T^{1,n} + E_T^{2,n} - U_{BE}^{1,n-1} - E_T^{2,n-1}}{\Delta t_n}) \\
& + \frac{1}{2}[(V^2, f(\cdot, t_n, U_T^{1,n} + E_T^{2,n})) + A(V^2, U_T^{1,n} + E_T^{2,n}) \\
& + (V^2, f(\cdot, t_{n-1}, U_{BE}^{1,n-1} + E_T^{2,n-1})) + A(V^2, U_{BE}^{1,n-1} + E_T^{2,n-1})] = 0, \\
& \text{for all } V^2 \in S_0^{N,2}.
\end{aligned} \tag{16c}$$

Temporal error estimation is local; thus, we use $U_{BE}^{1,n-1}$ as an initial condition for the trapezoidal rule integrations in Eqs. (16b) and (16c). Nodal superconvergence and the hierarchical formulation has uncoupled the piecewise linear and quadratic components of $U_T^{2,n}$. The spatial error estimate $E_T^{2,n}$ on the subinterval (x_{i-1}, x_i) is furthermore uncoupled from the error on other subintervals and this significantly reduces the computational complexity associated with solving Eq. (16c). The solution of Eq. (16b), noted in step (2), is necessary in order to increase the temporal accuracy of the solution because superconvergence only increases the order of accuracy in space. Some computational savings can generally be obtained, especially for nonlinear problems, by calculating $U_T^{1,n}$ as a defect correction to the backward Euler solution $U_{BE}^{1,n}$.

As described above,

$$\bar{e}^n := \|U_T^{1,n} + E_T^{2,n} - U_{BE}^{1,n}\|_1 \tag{17}$$

furnishes an estimate to the error $\|u - U_{BE}^{1,n}\|_1$ of the backward Euler solution. Equation (17) suggests the inequality

$$\bar{e}^n \leq \|U_T^{1,n} - U_{BE}^{1,n}\|_1 + \|E_T^{2,n}\|_1. \tag{18}$$

The term $\|U_T^{1,n} - U_{BE}^{1,n}\|_1$ is the difference between two piecewise linear solutions computed with temporal integration schemes of different orders and can be regarded as a measure of the temporal discretization error. In a similar

manner, $\|E_T^{2,n}\|_1$ can be regarded as a measure of the spatial discretization. Indeed, when the finite element system, Eq. (7), is integrated exactly in time, Adjerid and Flaherty (ref 6) proved that $\|E^2\|_1$ converges to the exact spatial discretization error $\|u - U^1\|_1$ as $N \rightarrow \infty$ for linear parabolic problems.

We conclude this section by presenting an example that indicates that \bar{e}^n , $\|U_T^{1,n} - U_{BE}^{1,n}\|_1$, and $\|E_T^{2,n}\|_1$ provide good estimates of the total, temporal, and spatial discretization errors, respectively.

Example 1: Consider the linear heat conduction problem

$$u_t = u_{xx}/\pi^2, \quad 0 < x < 1, \quad t > 0, \quad (19a)$$

$$u(x,0) = \sin \pi x, \quad 0 \leq x \leq 1, \quad (19b)$$

$$u(0,t) = u(1,t) = 0, \quad t > 0. \quad (19c,d)$$

The exact solution of this simple problem is

$$u(x,t) = e^{-t} \sin \pi x \quad (20)$$

We solved Eq. (19) on a uniform mesh with N finite elements for one time step Δt using the methods described above and several choices of N and Δt . The effectivity index

$$\theta := \bar{e}^1 / \|u(\cdot, \Delta t) - U_{BE}^{1,1}\|_1 \quad (21)$$

(see Reference 15), is used as a means of gaging the accuracy of the error estimate \bar{e}^1 . Ideally, we would like θ not to differ appreciably from unity and to approach unity as $N \rightarrow \infty$ and $\Delta t \rightarrow 0$.

We present a summary of results for the reciprocal of the effectivity index for a sequence of calculations performed with $N = 2^{p+1}$ and $\Delta t = 5^{-p/2}$, $p = 0, 1, \dots, 5$, in Figure 1. These results strongly suggest that $\theta \rightarrow 1$ as $p \rightarrow \infty$.

We use the temporal effectivity index

$$\theta_t := \|U_T^{1,1} - U_{BE}^{1,1}\|_1 / \|u(\cdot, \Delta t) - U_{BE}^{1,1}\|_1 \quad (22)$$

as a method of appraising the accuracy of the temporal error estimate $\|U_T^{1,1} - U_{BE}^{1,1}\|_1$. For fixed Δt , $\theta_t \rightarrow K_t(\Delta t)$ as $N \rightarrow \infty$ and the limiting value $K_t(\Delta t) \rightarrow 1$ as $\Delta t \rightarrow 0$.

We solve Eq. (19) for a single time step using a sequence of meshes with $N = 2^p$, $p = 3, 4, \dots, 10$, finite elements and time steps of $\Delta t = 0.7, 0.49, 0.343$, and 0.2401 . We present our findings for the temporal effectivity index θ_t as a function of p for the four time steps in Figure 2. As expected, θ_t tends to a limiting value $K_t(\Delta t)$ for large N , which approaches unity as $\Delta t \rightarrow 0$.

Finally, we define the spatial effectivity index as

$$\theta_s := \|E_T^{2,1}\|_1 / \|u(\cdot, \Delta t) - U_{BE}^{1,1}\|_1 \quad (23)$$

and use it as a measure of the spatial error estimate $\|E_T^{2,1}\|_1$. For fixed N , $\theta_s \rightarrow K_s(N)$ as $\Delta t \rightarrow 0$ and the limiting value $K_s(N) \rightarrow 1$ as $N \rightarrow \infty$.

Again, we solve Eq. (19) and present results for the reciprocal of the spatial effectivity index as a function of $\Delta t = 5^{-p/2}$, $p = 1, 2, \dots, 7$, for meshes with $N = 2, 4$, and 8 finite elements. These results suggest that for a fixed N , $\theta_s \rightarrow K_s(N)$ as $p \rightarrow \infty$, and that $K_s(N)$ is reasonably close to unity. Furthermore, it appears that $K_s(N) \rightarrow 1$ as N increases.

MESH REFINEMENT

The error estimates developed in the preceding paragraphs are used to control a simple global mesh refinement procedure that keeps \bar{e}^n below a specified tolerance TOL. Suppose that a solution $U_{BE}^{1,n-1}$ and error estimates $E_T^{2,n-1}$ and \bar{e}^{n-1} have been calculated at time t_{n-1} using a mesh with N elements and time step Δt_{n-1} . Further suppose that $\bar{e}^{n-1} < \text{TOL}$ and calculate solutions and error estimates at time $t_n = t_{n-1} + \Delta t_n$ using a mesh with N elements and time step $\Delta t_n = \Delta t_{n-1}$. Our refinement strategy consists of checking \bar{e}^n and proceeding as follows:

- (1) if $\bar{e}^n \leq \text{TOL}$, continue to the next time step;
- (2) if $\bar{e}^n > \text{TOL}$, and $0.3 < \|E_T^{2,n}\|/\bar{e}^n < 0.7$, double N , reduce Δt_n by 30 percent, and redo the integration;
- (3) if $\bar{e}^n > \text{TOL}$ and $0.7 \leq \|E_T^{2,n}\|/\bar{e}^n$, double N and redo the integration;
and
- (4) if $\bar{e}^n > \text{TOL}$ and $\|E_T^{2,n}\|/\bar{e}^n \leq 0.3$, reduce Δt_n by 30 percent and redo the integration.

Steps (2) through (4) are repeated until step (1) is satisfied.

The main advantage of this refinement procedure is that the separate estimates of the spatial and temporal errors allow different strategies to be used depending upon the dominant component of the error. Thus, if the spatial component of the error, as measured by $\|E_T^{2,n}\|/\bar{e}^n$ is large, then only spatial refinement is used to reduce the total error. The opposite situation arises when the spatial component of the error is small.

It is important to note that the error estimates used in the refinement procedure are, at best, only asymptotically correct. Thus, they will not produce reliable estimates on coarse meshes or when errors are large. With this in mind, it may be best to replace \bar{e}^n by $\|U_T^{1,n} - U_{BE}^{1,n}\|_1 + \|E_T^{2,n}\|_1$ in the refinement procedure.

The specific choice of the limiting values 0.3 and 0.7 that are used to determine the dominant component of the error in our refinement procedure are basically arbitrary. Under normal circumstances, the spatial error measure $\|E_T^{2,n}\|/\bar{e}^n \in (0,1)$; thus, it is reasonable to divide $(0,1)$ approximately into thirds, i.e., $(0,0.3)$, $(0.3,0.7)$, and $(0.7,1)$ corresponding, respectively, to only temporal refinement, temporal and spatial refinement, and only spatial

refinement. This strategy may not be appropriate in all situations and further analysis and experimentation is needed to determine optimal refinement criteria.

A local refinement strategy, such as those considered in References 2,4-6,8-12, is usually more efficient than the global strategy presented herein. Our plans are to combine refinement with a mesh moving method that equidistributes a global error measure on a mesh with a fixed number of finite elements (refs 16,17). It may be possible to use a simple global refinement strategy in conjunction with such a mesh moving method since the local error measure will be approximately the same on every subinterval.

Doubling the number of finite elements whenever spatial refinement is performed simplifies interpolation issues, but may add more nodes than necessary. Reducing the time step by 30 percent keeps temporal accuracy comparable to spatial accuracy, since the temporal convergence rate is $O(\Delta t_n^2)$, while the spatial convergence rate is $O(1/N)$. Thus, doubling N would correspond to reducing Δt_n by $1/\sqrt{2}$, which is approximately 30 percent.

We apply the above refinement procedure to the following singular parabolic problem.

Example 2: Consider the partial differential system

$$u_t + u/[2(1-t)] = -u_{xx}/4, \quad 0 < x < \infty, \quad 0 < t < 1, \quad (24a)$$

$$u(x,0) = e^{-x^2}, \quad 0 \leq x < \infty, \quad (24b)$$

$$u_x(0,t) = \lim_{s \rightarrow \infty} u_x(s,t) = 0, \quad 0 < t < 1. \quad (24c,d)$$

The exact solution of this problem is

$$u(x,t) = e^{-x^2/(1-t)}. \quad (25)$$

This problem was motivated by our interest in solving the nonlinear Schrödinger equation in cylindrical coordinates (ref 18). It is known (ref 19) that the solution of the Schrödinger equation can "self-focus," i.e., its

solution can become infinite at one point, while decaying elsewhere on the domain. Problems of this type occur in laser optics.

Such problems are difficult to solve by traditional numerical methods and illustrate the need for adaptive strategies. The model given by Eq. (24) was developed as a simple approximation of the behavior of the Schrödinger equation. Its solution "focuses" in the sense that $u(x,t) \rightarrow 0$, $x > 0$, as $t \rightarrow 1$, while $u(0,t) = 1$.

This problem was solved for values of TOL of 0.2, 0.1, and 0.05 and a summary of the results are presented in Tables I, II, and III, respectively. These tables present the relevant refinement data for each time step of the solution process. The time and numerical parameters Δt and N at the beginning of a solution step are found in the columns labelled "Initial Time," "Initial Δt ," and "Initial N ," respectively. The refined values of Δt and N , necessary to complete the solution step within the given tolerance, are found in the columns labelled "Refined Δt ," and "Refined N ," respectively. The resulting time at the end of a solution step is found in the column labelled "Final Time." The last column, labelled "Total Error Estimate," lists the value of \bar{e}^n at the successful completion of a time step. The rows of each table outline the solution process as it advances through time.

These results indicate that it is sometimes possible to reduce the total error by refining only in space or only in time, and that the error estimates \bar{e}^n , $\|U_T^{1,n} - U_{BE}^{1,n}\|_1$, and $\|E_T^{2,n}\|_1$ can be used to detect when these situations arise.

TABLE I. NUMERICAL PARAMETERS AT THE BEGINNING AND THE END OF EACH TIME STEP FOR SOLVING EXAMPLE 2 WITH TOL = 0.2

Initial Time	Initial Δt	Initial N	Refined Δt	Refined N	Final Time	Total Error Estimate
0.0000	0.1250	16	0.1250	16	0.1250	0.0885
0.1250	0.1250	16	0.1250	16	0.2500	0.1496
0.2500	0.1250	16	0.0875	32	0.3375	0.1062
0.3375	0.0875	32	0.0875	32	0.4250	0.1931
0.4250	0.0875	32	0.0613	64	0.4863	0.1381
0.4863	0.0613	64	0.0429	128	0.5291	0.0782
0.5291	0.0429	128	0.0429	128	0.5720	0.1144
0.5720	0.0429	128	0.0429	128	0.6149	0.1404
0.6149	0.0429	128	0.0429	128	0.6578	0.1911
0.6578	0.0429	128	0.0300	256	0.6878	0.1052

TABLE II. NUMERICAL PARAMETERS AT THE BEGINNING AND THE END OF EACH TIME STEP FOR SOLVING EXAMPLE 2 WITH TOL = 0.1

Initial Time	Initial Δt	Initial N	Refined Δt	Refined N	Final Time	Total Error Estimate
0.0000	0.1250	16	0.1250	16	0.1250	0.0885
0.1250	0.1250	16	0.0875	32	0.2125	0.0496
0.2125	0.1250	32	0.0875	32	0.3000	0.0615
0.3000	0.0875	32	0.0613	64	0.3613	0.0390
0.3613	0.0613	64	0.0613	64	0.4225	0.0549
0.4225	0.0613	64	0.0429	64	0.4654	0.0604
0.4654	0.0429	64	0.0300	128	0.4954	0.0340
0.4954	0.0300	128	0.0300	128	0.5254	0.0528
0.5254	0.0300	128	0.0300	128	0.5554	0.0847
0.5554	0.0300	128	0.0210	128	0.5764	0.0782

TABLE III. NUMERICAL PARAMETERS AT THE BEGINNING AND THE END OF EACH TIME STEP FOR SOLVING EXAMPLE 2 WITH TOL = 0.5

Initial Time	Initial Δt	Initial N	Refined Δt	Refined N	Final Time	Total Error Estimate
0.0000	0.1250	16	0.1250	32	0.1250	0.0451
0.1250	0.1250	32	0.0875	64	0.2125	0.0261
0.2125	0.0875	64	0.0875	64	0.3000	0.0377
0.3000	0.0875	64	0.0613	64	0.3613	0.0375
0.3613	0.0613	64	0.0429	128	0.4041	0.0211
0.4041	0.0429	128	0.0429	128	0.4470	0.0300
0.4470	0.0429	128	0.0300	256	0.4470	0.0176
0.5070	0.0300	256	0.0210	256	0.5280	0.0202
0.5280	0.0210	256	0.0210	256	0.5490	0.0272

DISCUSSION

We developed methods for calculating a posteriori estimates of the total, spatial, and temporal discretization errors when a vector system of parabolic partial differential equations is solved using piecewise linear finite elements in space and the backward Euler method in time. The error estimates are obtained by using higher order methods, with nodal superconvergence being used to improve computational efficiency.

The three estimates were used to control a global refinement procedure that attempts to keep a global measure of the error per time step below a prescribed tolerance. Refinement can be performed in space, time, or both space and time depending on the dominant component of the error estimate.

Comparison of the exact and estimated errors, presented in Example 1, give us some confidence in the accuracy of our error estimates. Additionally, the results of Example 2 provide an indication of the utility of these estimates in

an adaptive procedure. In certain situations, only spatial or temporal refinement was needed to keep the total error within the prescribed tolerance, and our error estimates could be used to determine when these situations arise.

This is the first attempt that we know of which simultaneously addresses spatial and temporal errors with different refinement strategies. Some researchers (refs 8-11) have used binary refinement in space and time, but did not attempt to determine the dominant component of the total discretization error. As noted, method of lines techniques (refs 1,2,4,5) typically assume that temporal integration is exact and refine based on estimates of spatial errors. There is a great potential for techniques that utilize different spatial and temporal refinement strategies, particularly with problems having singularities. Our work, however, is still very preliminary and there is still a great deal to be done. Rigorous convergence results for our error estimates are yet to be established. The refinement algorithm previously discussed is very simple and will likely benefit from further experimental and theoretical analyses. We also anticipate that the inclusion of a mesh moving procedure based on equidistributing a global error measure (ref 16) will dramatically improve the performance of our adaptive solution technique. In the future, we would like to extend our techniques to multi-dimensional problems and to consider higher order spatial and temporal discretization methods.

REFERENCES

1. S. Adjerid and J. E. Flaherty, "A Moving Finite Element Method With Error Estimation and Refinement for One-Dimensional Time Dependent Partial Differential Equations," SIAM J. Numer. Anal., Vol. 23, 1986, pp. 778-796.
2. S. Adjerid and J. E. Flaherty, "A Moving Mesh Finite Element Method With Local Refinement For Parabolic Partial Differential Equations," Comp. Meths. Appl. Mech. Engr., Vol. 56, 1986, pp. 3-26.
3. L. R. Petzold, "A Description of DASSL: A Differential/Algebraic System Solver," Sandia Report No. Sand. 82-8637, Sandia National Laboratory, Livermore, CA, 1982.
4. M. Bieterman and I. Babuska, "The Finite Element Method For Parabolic Equations, I: A Posteriori Error Estimation," Numer. Math., Vol. 40, 1982, pp. 339-371.
5. M. Bieterman and I. Babuska, "The Finite Element Method For Parabolic Equations, II: A Posteriori Error Estimation and Adaptive Approach," Numer. Math., Vol. 40, 1982, pp. 373-406.
6. S. Adjerid and J. E. Flaherty, "Local Refinement Finite Element Methods on Stationary and Moving Meshes For One-Dimensional Parabolic Systems," in preparation.
7. C. W. Gear, Numerical Initial Value Problems in Ordinary Differential Equations, Prentice-Hall, Englewood Cliffs, NJ, 1971.
8. M. Berger and J. Oliger, "Adaptive Mesh Refinement For Hyperbolic Partial Differential Equations," J. Comput. Phys., Vol. 53, 1984, pp. 484-512.
9. M. Berger, "Data Structures For Adaptive Mesh Refinement," in Adaptive Computational Methods For Partial Differential Equations, (I. Babuska, J. Chandra, J. E. Flaherty, eds.), SIAM, Philadelphia, 1983.
10. M. Bieterman, J. E. Flaherty, and P. K. Moore, "Adaptive Local Refinement Methods For Nonlinear Parabolic Partial Differential Equations," in Accuracy Estimates and Adaptive Refinements in Finite Element Computations, (I. Babuska, O. C. Zienkiewicz, J. R. Gago, and E. R. de A. Olivera, eds.), John Wiley and Sons, Chichester, England, 1986, Chapter 19.
11. J. E. Flaherty and P. K. Moore, "A Local Refinement Finite Element Method For Time Dependent Partial Differential Equations," Transactions of the Second Army Conference on Applied Mathematics and Computing, ARO Report 85-1, US Army Research Office, Research Triangle Park, NC, 1985, pp. 585-596.
12. D. Gannon, "Self Adaptive Methods For Parabolic Partial Differential Equations," Ph.D. Thesis, Department of Computer Science, University of Illinois at Urbana-Champaign, 1980.

13. V. Thomee, "Negative Norm Estimates and Superconvergence in Galerkin Methods for Parabolic Problems," Math. Comp., Vol. 34, 1980, pp. 93-113.
14. G. Strang and G. Fix, An Analysis of the Finite Element Method, Prentice-Hall, Englewood Cliffs, NJ, 1973.
15. I. Babuska, A. Miller, and M. Vogelius, "Adaptive Methods and Error Estimation For Elliptic Problems of Structural Mechanics," in Adaptive Computational Methods For Partial Differential Equations, (I. Babuska, J. Chandra, J. E. Flaherty, eds.), SIAM, Philadelphia, pp. 57-73.
16. J. M. Coyle, J. E. Flaherty, and R. Ludwig, "On the Stability of Mesh Equidistribution Strategies For Time-Dependent Partial Differential Equations," J. Comput. Phys., Vol. 62, 1986, pp. 26-39.
17. S. Davis and J. E. Flaherty, "An Adaptive Finite Element Method For Initial-Boundary Value Problems For Partial Differential Equations," SIAM J. Sci. Stat. Comput., Vol. 3, 1982, pp. 6-27.
18. J. E. Flaherty, J. M. Coyle, R. Ludwig, and S. F. Davis, "Adaptive Finite Element Methods For Parabolic Partial Differential Equations," in Adaptive Computational Methods For Partial Differential Equations, (I. Babuska, J. Chandra, and J. E. Flaherty, eds.), SIAM, Philadelphia, 1983, pp. 144-164.
19. K. Konno and H. Suzuki, "Self-Focusing of Laser Beams in Nonlinear Media," Physica Scripta, Vol. 20, 1979, pp. 382-386.

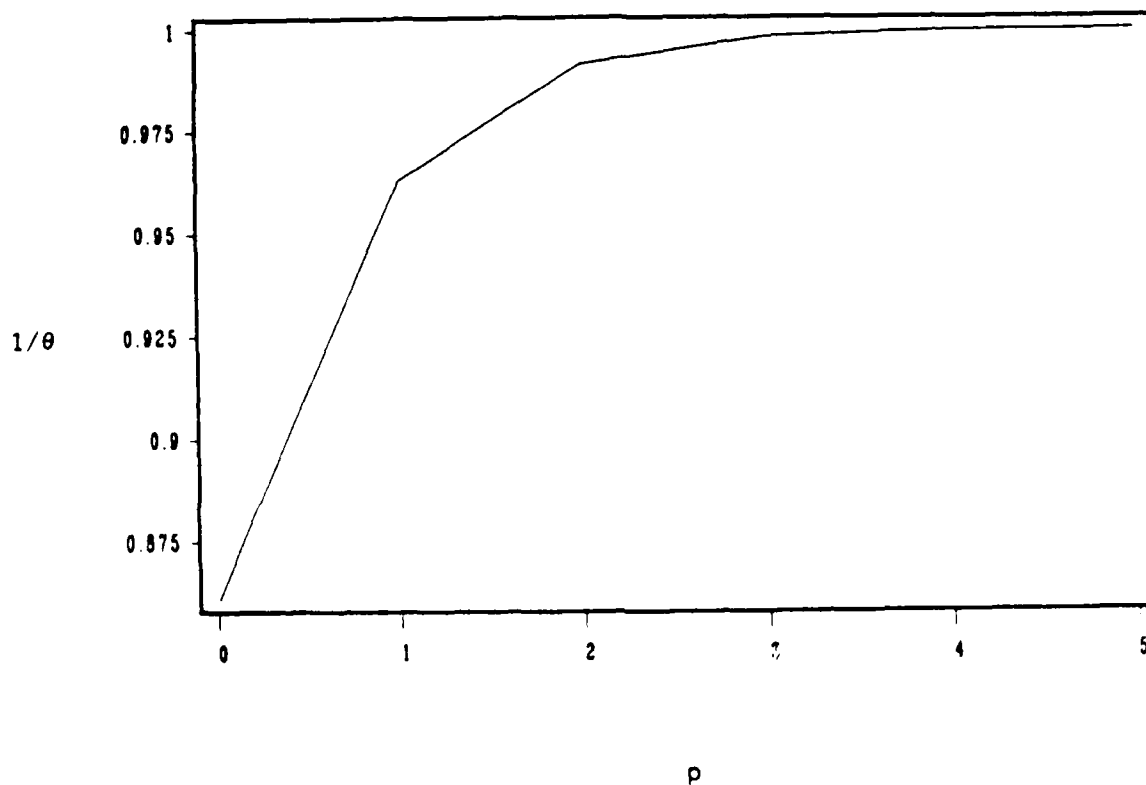


Figure 1. Reciprocal of the effectivity index θ versus p , where $N = 2^{p+1}$ and $\Delta t = 5^{-p}/2$ when solving Example 1. Note that θ approaches 1 as p increases.

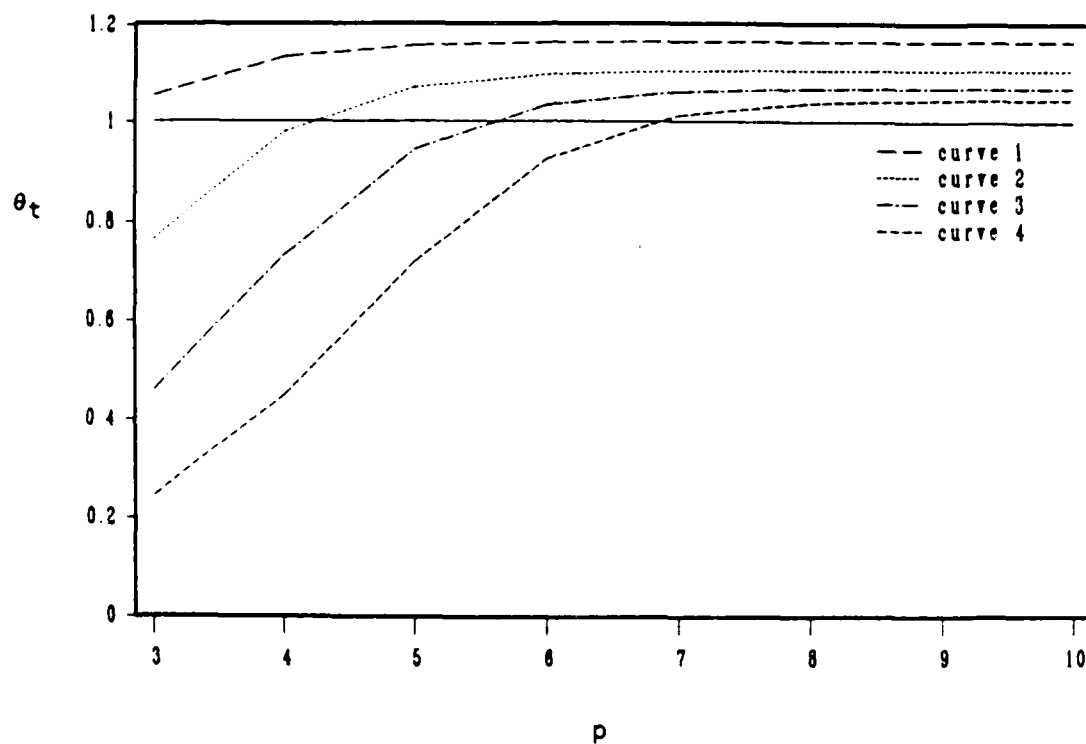


Figure 2. Temporal effectivity index θ_t for $\Delta t = 0.7$ (curve 1), $\Delta t = 0.49$ (curve 2), $\Delta t = 0.343$ (curve 3), and $\Delta t = 0.2401$ (curve 4), versus p , where $N = 2^p$ when solving Example 1. Note that θ_t approaches 1 as Δt decreases.

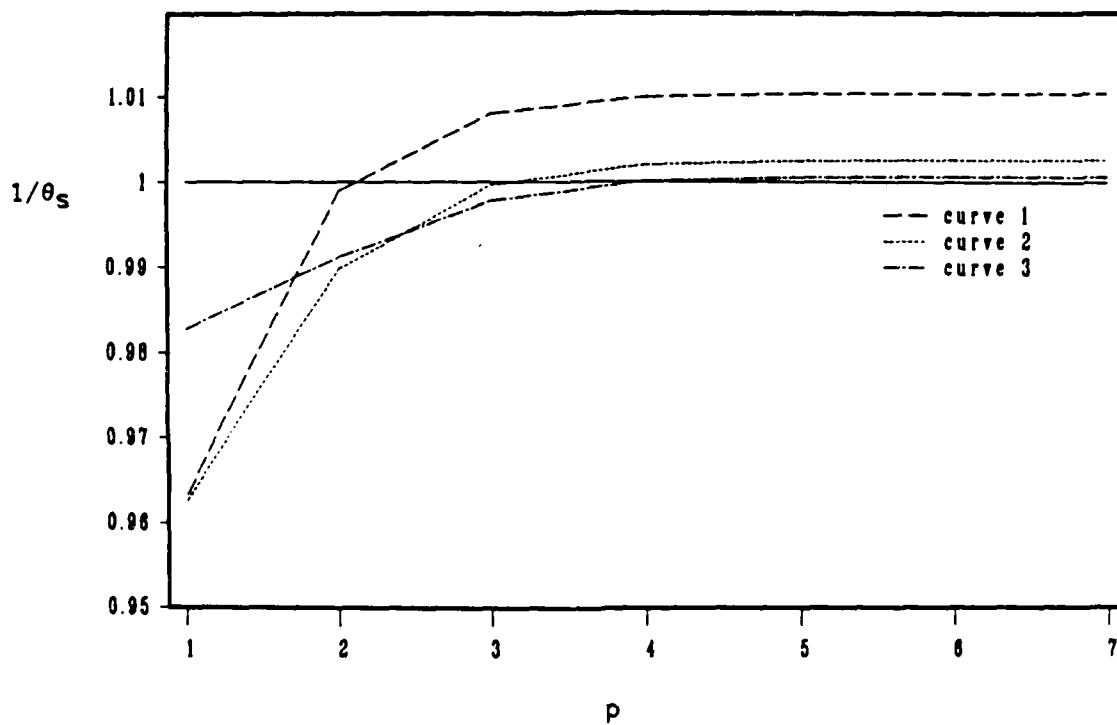


Figure 3. Reciprocal of the spatial effectivity index θ_s for $N = 2$ (curve 1), $N = 4$ (curve 2), and $N = 8$ (curve 3) versus p , where $\Delta t = 5^{-p}/2$ when solving Example 1. Note that θ_s approaches 1 as N increases.

TECHNICAL REPORT INTERNAL DISTRIBUTION LIST

	<u>NO. OF COPIES</u>
CHIEF, DEVELOPMENT ENGINEERING BRANCH	
ATTN: SMCAR-CCB-D	1
-DA	1
-DC	1
-DM	1
-DP	1
-DR	1
-DS (SYSTEMS)	1
CHIEF, ENGINEERING SUPPORT BRANCH	
ATTN: SMCAR-CCB-S	1
-SE	1
CHIEF, RESEARCH BRANCH	
ATTN: SMCAR-CCB-R	2
-R (ELLEN FOGARTY)	1
-RA	1
-RM	1
-RP	1
-RT	1
TECHNICAL LIBRARY	5
ATTN: SMCAR-CCB-TL	
TECHNICAL PUBLICATIONS & EDITING UNIT	2
ATTN: SMCAR-CCB-TL	
DIRECTOR, OPERATIONS DIRECTORATE	1
ATTN: SMCWV-OD	
DIRECTOR, PROCUREMENT DIRECTORATE	1
ATTN: SMCWV-PP	
DIRECTOR, PRODUCT ASSURANCE DIRECTORATE	1
ATTN: SMCWV-QA	

NOTE: PLEASE NOTIFY DIRECTOR, BENET LABORATORIES, ATTN: SMCAR-CCB-TL, OF ANY ADDRESS CHANGES.

TECHNICAL REPORT EXTERNAL DISTRIBUTION LIST

	<u>NO. OF COPIES</u>		<u>NO. OF COPIES</u>
ASST SEC OF THE ARMY RESEARCH AND DEVELOPMENT ATTN: DEPT FOR SCI AND TECH THE PENTAGON WASHINGTON, D.C. 20310-0103	1	COMMANDER ROCK ISLAND ARSENAL ATTN: SMCRI-ENM ROCK ISLAND, IL 61299-5000	1
ADMINISTRATOR DEFENSE TECHNICAL INFO CENTER ATTN: DTIC-FDAC CAMERON STATION ALEXANDRIA, VA 22304-6145	12	DIRECTOR US ARMY INDUSTRIAL BASE ENGR ACTV ATTN: AMXIB-P ROCK ISLAND, IL 61299-7260	1
COMMANDER US ARMY ARDEC ATTN: SMCAR-AEE	1	COMMANDER US ARMY TANK-AUTMV R&D COMMAND ATTN: AMSTA-DDL (TECH LIB) WARREN, MI 48397-5000	1
SMCAR-AES, BLDG. 321	1	COMMANDER US MILITARY ACADEMY ATTN: DEPARTMENT OF MECHANICS WEST POINT, NY 10996-1792	1
SMCAR-AET-O, BLDG. 351N	1		
SMCAR-CC	1		
SMCAR-CCP-A	1		
SMCAR-FSA	1		
SMCAR-FSM-E	1	US ARMY MISSILE COMMAND REDSTONE SCIENTIFIC INFO CTR ATTN: DOCUMENTS SECT, BLDG. 4484 REDSTONE ARSENAL, AL 35898-5241	2
SMCAR-FSS-D, BLDG. 94	1		
SMCAR-MSI (STINFO)	2		
PICATINNY ARSENAL, NJ 07806-5000			
DIRECTOR US ARMY BALLISTIC RESEARCH LABORATORY ATTN: SLCBR-DD-T, BLDG. 305 ABERDEEN PROVING GROUND, MD 21005-5066	1	COMMANDER US ARMY FGN SCIENCE AND TECH CTR ATTN: DRXST-SD 220 7TH STREET, N.E. CHARLOTTESVILLE, VA 22901	1
DIRECTOR US ARMY MATERIEL SYSTEMS ANALYSIS ACTV ATTN: AMXSY-MP ABERDEEN PROVING GROUND, MD 21005-5071	1	COMMANDER US ARMY LABCOM MATERIALS TECHNOLOGY LAB ATTN: SLCMT-IML (TECH LIB) WATERTOWN, MA 02172-0001	2
COMMANDER HQ, AMCCOM ATTN: AMSMC-IMP-L ROCK ISLAND, IL 61299-6000	1		

NOTE: PLEASE NOTIFY COMMANDER, ARMAMENT RESEARCH, DEVELOPMENT, AND ENGINEERING CENTER, US ARMY AMCCOM, ATTN: BENET LABORATORIES, SMCAR-CCB-TL, WATERVLIET, NY 12189-4050, OF ANY ADDRESS CHANGES.

TECHNICAL REPORT EXTERNAL DISTRIBUTION LIST (CONT'D)

	<u>NO. OF COPIES</u>		<u>NO. OF COPIES</u>
COMMANDER US ARMY LABCOM, ISA ATTN: SLCIS-IM-TL 2800 POWDER MILL ROAD ADELPHI, MD 20783-1145	1	COMMANDER AIR FORCE ARMAMENT LABORATORY ATTN: AFATL/MN EGLIN AFB, FL 32543-5434	1
COMMANDER US ARMY RESEARCH OFFICE ATTN: CHIEF, IPO P.O. BOX 12211 RESEARCH TRIANGLE PARK, NC 27709-2211	1	COMMANDER AIR FORCE ARMAMENT LABORATORY ATTN: AFATL/MNF EGLIN AFB, FL 32542-5000	1
DIRECTOR US NAVAL RESEARCH LAB ATTN: MATERIALS SCI & TECH DIVISION CODE 26-27 (DOC LIB) WASHINGTON, D.C. 20375	1 1	METALS AND CERAMICS INFO CTR BATTELLE COLUMBUS DIVISION 505 KING AVENUE COLUMBUS, OH 43201-2693	1

NOTE: PLEASE NOTIFY COMMANDER, ARMAMENT RESEARCH, DEVELOPMENT, AND ENGINEERING CENTER, US ARMY AMCCOM, ATTN: BENET LABORATORIES, SMCAR-CCB-TL, WATERVLIET, NY 12189-4050, OF ANY ADDRESS CHANGES.

END
DATE
FILMED

4-88

DTIC